

The influence of temperature on the dynamics of protein precrystallization clusters, studied by photon correlation spectroscopy

Wolfram Eberstein, Yannis Georgalis, Wolfram Saenger

Institut für Kristallographie, Freie Universität Berlin, Takusstrasse 6, D-14195 Berlin, Germany

Received: 3 June 1993 / Accepted in revised form: 24 August 1993

Abstract. Hen-egg white lysozyme was used for studying the influence of temperature on crystallization. The reaction was initiated at variable temperatures, covering the range between 5–50 °C, and was monitored with photon correlation spectroscopy. When aggregation was induced by addition of NaCl, the clusters formed exhibited diffusion limited aggregation behavior and crystals appeared in less than two days. In contrast, $(\text{NH}_4)_2\text{SO}_4$ induced aggregation took place mostly in the cross-over regime. In this case, solutions either remained transparent and void of crystals or formed gels within a few weeks. In both cases the kinetics could be dynamically scaled into master curves indicating that the precrystallization formed aggregates are fractals resulting from different collision processes.

Key words: Fractal cluster growth – Protein crystal growth – Photon correlation spectroscopy

1. Introduction

Few attempts have been made to elucidate the sequence of events involved in protein crystallization (Boistelle and Astier 1988) and the field still lacks a coherent description since precise kinetic data are unavailable for proteins. At the descriptive level, major deviations are not expected to occur upon comparison with inorganic materials (Rosenberger 1986). However, the absence of suitable observables renders rigorous physical-chemical foundations difficult. In recent years, this pitfall has been recognized by protein crystallographers and light scattering techniques rapidly gain ground in the elucidation and early diagnosis of the protein crystallization process.

The fate of the protein solution is expected to depend on the nature of events during the very early stages of the aggregation process. Cluster formation kinetics can be treated according to contemporary fractal aggregation

theory (Weitz and Lin 1986; Meakin 1988; Vicsek 1989; Klein et al. 1990; Kolb 1991). Recent progress in these disciplines came from developments of scaling theories and the further notion that fractal growth provides efficient means to describe quantitatively aggregation processes.

We have shown that the initial growth process is accompanied by the formation of large fractal structures (Georgalis et al. 1992; 1993) resulting from different collision processes. In this work we have investigated the influence of starting temperature on the formation of precrystallization aggregates. In this work we will show that the formation of precrystallization aggregates and the long-time behavior of the solutions is a very delicate function of the temperature applied at the initial stages. Differences in the precursors growth process are associated with the crystal formation of lysozyme.

1.1. Photon correlation spectroscopy

The theory of PCS has been reviewed by Schmitz (1990) and Chu (1991). Therefore only elementary considerations need to be presented at this point. As a highly idealized case we will consider an interaction free, monodisperse ensemble of spherical particles undergoing Brownian motion as a consequence of the thermal agitation of the solvent. Laser light scattered from these particles is received in the direction of the scattering angle θ by a photomultiplier. The Brownian motion of the particles leads to Doppler broadening and the scattered light is characterized by a linewidth increase compared to the incoming laser light. The increase is very small, typically in the KHz range and therefore cannot be resolved by gratings or interferometric techniques. This small linewidth corresponds to slow fluctuations of the scattered intensity typically in the ms range. If the size of the particles is very small in comparison with the wavelength of incident light, the scattered intensity will fluctuate around a mean value

$$I(t) = \sum_k a_k e^{i\mathbf{q}\cdot\mathbf{r}_k(t)}. \quad (1)$$

In Eq. (1) \mathbf{r}_k denotes the position of the k -th particle in space and a_k is its scattering amplitude. The spatial resolution of experiments is defined by the scattering vector \mathbf{q} whose magnitude is given by the Bragg formula

$$q = |\mathbf{q}| = \frac{4\pi n_0}{\lambda} \sin(\theta/2), \quad (2)$$

where λ is the wavelength of the laser beam and n_0 the refractive index of the suspending medium.

The first order autocorrelation function (ACF) can be written as

$$G^{(1)}(\tau) = \left\langle \sum_k (a_k)^2 e^{i\mathbf{q}[\mathbf{r}_k(t) - \mathbf{r}_k(t-\tau)]} \right\rangle, \quad (3)$$

where the angular brackets denotes time average and the vector $\mathbf{r}_k(t) - \mathbf{r}_k(t-\tau)$ the displacement of the k -th particle due to Brownian motion in time τ (Einstein 1905, 1906).

$$\langle (\mathbf{r}_k(t) - \mathbf{r}_k(t-\tau))^2 \rangle = 6D_T\tau. \quad (4)$$

Combining Eqs. (3) and (4) the field ACF can be written as

$$G^{(1)}(\tau) = \sum_k (a_k)^2 e^{-D_T q^2 \tau}. \quad (5)$$

Experimentally the intensity or second order correlation function is the measured quantity. It is related to the first order correlation function via the relation (Siebert 1943)

$$G^{(2)}(\tau) = (G^{(1)}(0))^2 + |G^{(1)}(\tau)|^2. \quad (6)$$

Combining Eqs. (5) and (6) we obtain for the intensity ACF function

$$G^{(2)}(\tau) = (\sum_k a_k^2)^2 (1 + e^{-2D_T q^2 \tau}) \quad (7)$$

that can be fit to an intensity correlation function which can be obtained from a modern PCS spectrometer. Output signals are transferred to a digital correlator (for reviews see Schulz-Dubois 1983; Schätzel 1993) where after amplification and discrimination the necessary operations are carried out. For monodisperse solutions a simple semilogarithmic expansion of the ACF yields the z -average translational diffusion coefficient D_T . The mean hydrodynamic radius R_h of the particle can then be readily obtained from the Stokes-Einstein relation

$$D_T = \frac{k_B T}{6\pi\eta R_h} \quad (8)$$

where k_B denotes Boltzmann's constant, T absolute temperature, and η the viscosity of the medium, respectively.

In the examined systems samples usually depart from the dilute regime, are not monodisperse, cannot be treated as hard impermeable spheres and their size becomes larger than the wavelength of the incoming light after a few minutes. The ACF is a superposition of exponentials characterized by a distribution of relaxation times and scattering amplitudes proportional to the light scattered by each species. More complex, albeit tractable by contemporary evaluation schemes, formulation of the ACF holds for polydisperse systems (Lindsay et al. 1988, 1989). In this case an integration over the cluster size distribution $N(R)$ is involved. Equation (7) can be written in a

form that allows one to account for polydispersity (Lin et al. 1990 a, b)

$$G^{(2)}(\tau) \propto \int N(R) M^2(R) S(qR) e^{-hR^{-1}q^2\tau} dR \quad (9)$$

where h is a proportionality constant, $M(R)$ is the mass and $S(qR)$ the static structure factor of a cluster having a radius R . The resolution of sums of exponentials is known to comprise an ill-conditioned problem and renders data analysis difficult. All these deviations from the ideal case pose severe restrictions in the experimental design, data acquisition and concomitant evaluation procedures. Furthermore, fractals are asymmetric structures, and the contributions of both translational and rotational modes into R_{eff} , must be considered if $qR > 0.2$. The field ACF of anisotropic, inhomogeneous scatterers have been calculated with the assumption that rotational and translational motions are uncoupled (Lindsay et al. 1988, 1989). Computer generated and experimentally produced diffusion limited aggregates show typical asymmetry ratios of about 1.7, a value that indicates that this assumption applies. Numerical expressions for the structure factors of fractal clusters have been obtained (Lin et al. 1990a, b). These advances allow for precise assessments of the cluster size kinetics (Klein et al. 1990).

1.2. Fractal cluster aggregation regimes

When particles associate, low density, random structures very often result. These structures can be described as fractal clusters. Their formation by non-equilibrium processes has been studied extensively in recent years, especially by computer simulations and scattering techniques (Vicsek 1989; Kolb 1991; Martin and Ackerson 1985; Martin and Leyvraz 1986). The simplest type is termed self-similar fractals. Such clusters are invariant to isotropic changes of the length scale, i.e. look the same when observed under different magnifications, and exhibit scaling symmetry.

For inorganic colloids two distinct fractal aggregation regimes with universal scaling properties are known. If the energy barrier is smaller than thermal energy, diffusion is the rate limiting step and each encounter leads to aggregation. This regime is termed diffusion limited cluster aggregation (DLCA) regime. The kinetics of cluster growth can then be described as follows (Weitz et al. 1984; Feder et al. 1984; Rarity et al. 1989)

$$R(t) = R_0 (1 + ct)^{1/d_f} \quad (10)$$

where

$$c = \alpha \frac{4k_B T}{3\eta} N_0 \quad (11)$$

$$= k_s N_0 \quad (12)$$

and R_0 is the monomer radius, d_f the fractal dimension and N_0 the total number of seed particles. In Eq. (10) c can be then recognized as the probability of collision and k_s as the Smoluchowski (1916, 1917) rate constant. The variable α denotes the sticking probability, α , defined in electrostatic theory as reciprocal stability factor of col-

loidal aggregation (Verwey and Overbeek 1948). Equation (10) involves the assumption that $\alpha = 1$ with unity.

If the repulsive energy barriers are sufficiently higher than the thermal energy, aggregates will be prevented from sticking upon collision and aggregation is termed as reaction limited cluster aggregation (RLCA). The growth kinetics follow in this case (Weitz et al. 1984; Weitz and Lin 1986; Ball et al. 1987) a diverging exponential law

$$R(t) = R_0 e^{c't} \quad (13)$$

where $c' = c\alpha$ and α should much smaller than unity for the pure RLCA regime.

Intermediate cases where both regimes manifest their properties in a mixed way are in generally called the cross-over regime. The latter regime is rich in information and of relevance in protein crystallization studies. Precise determination of the fractal dimension requires again the support of angular dependence light scattering measurements.

2. Materials and methods

2.1. Materials

All chemicals used in the present work were of analytical grade and water was obtained from a Millipore-Q device. Hen-egg white lysozyme, three times crystallized was purchased from Sigma Chemical Co. (Deisenhofen, Germany). Protein preparations were treated as previously described (Georgalis et al. 1993) dissolved in a 0.1 M Na-acetate buffer, pH 4.2 and tested for monodispersity with PCS in the absence of salt. The temperature dependence of the pH of this buffer is linear in the temperature range employed and the gradient $\Delta\text{pH}/\Delta T$ amounts to only 0.01 pH units. At the very extreme temperatures employed this variation will not cause drastic changes and pH has been considered constant throughout. Salts were purchased from Merck (Darmstadt, Germany), were of high purity and were always prepared fresh as concentrated stock solutions in the same buffer.

Protein and salt solutions were mixed in the appropriate ratio and filtered through Minisart (Sartorius GmbH, Germany) sterile filters, 0.22 μm pore size, into standard cylindrical light scattering cells. In all experiments we have employed a standard lysozyme concentration of 2.1 mM, unless otherwise stated. The concentration of NaCl throughout was 0.64 M, and that of $(\text{NH}_4)_2\text{SO}_4$ 1.14 M. The choice of these conditions is empirical and serves only as a reasonable balance between the total experimentation time and the appearance of the crystalline phase.

Viscosities of solution were experimentally determined as a function of temperature by employing an AVS/G viscosimeter facility (Schott, Mainz, Germany) and capillary Ostwald viscosimeters.

2.2. PCS – data acquisition and evaluation

PCS experiments were conducted with an ALV/SP-80 light scattering spectrogoniometer (ALV, Langen, Ger-

many) and the ALV-500/FAST digital correlator with 286 channels spaced quasi-logarithmically in time. A Spectraphysics 165 Ar⁺ laser operating at a wavelength of 488 nm served as light source. The scattering angle employed was in all cases 20°.

Temperatures in the range from 5 to 50.0°C were controlled by a Lauda RC6 thermostat with a nominal accuracy of $\pm 0.01^\circ\text{C}$. Experiments were initiated within less than 1 min after mixing of the solutions and triplicate measurements were performed at each temperature in order to reduce uncertainties. Owing to the rapid size increment of the clusters, the first thirty spectra were sampled over 30 s, whereas the next thirty over 60 s, unless otherwise stated. The elapsed time between two experiments was 4.5 s. The total time of a typical kinetic experiment was kept to equal to 3000 s.

The particle distribution function of clusters was obtained after Laplace inversion of the ACF with a modified version of the program CONTIN (Provencher 1982 a, b) implemented in a CONVEX-C200 supercomputer. Decoupling of the rotational modes and calculation of the appropriate structure factors were accomplished as previously described (Georgalis et al. 1993). Output files of CONTIN in reduced format were further manipulated with graphics and standard non-linear fitting routines for extracting the parameters of interest. Upon completion of the experiments the light scattering cells were stored in an air-conditioned crystallization room at 17.5°C and observed under a light microscope for a period of several weeks.

3. Results

NaCl is known to induce the crystal formation of lysozyme. We employed conditions for which we know a priori that temperatures between 17.5 and 20°C will lead to successful crystallization. In contrast $(\text{NH}_4)_2\text{SO}_4$ is not known to induce crystallization of lysozyme (Ries-Kautt and Ducruix 1989; Ducruix and Ries-Kautt 1990), whereas for more than 60% of protein crystals obtained so far it has played a deciding role (NIST data bank update 1992, described in Gilliland and Bickham 1990). We will demonstrate that these two agents influence in a different manner the initial aggregation stage and lead to completely diffusion final structures.

Employing either NaCl or $(\text{NH}_4)_2\text{SO}_4$ as precipitating agents, the cluster size reaches a point where the radius does not appreciably increase within the spectra accumulation time. We have introduced the term quasi-stationary hydrodynamic radius. The definition is arbitrary and denotes an average radius obtained from data in the range 2000 to 3000 s in a kinetic experiment. It serves for describing gross changes in the overall behavior of the clusters rather than absolute dimensions of the clusters in the particle sizing sense.

3.1. Aggregation kinetics

The mass of a fractal cluster scales according to a power law (Klein et al. 1990; Rarity et al. 1989; Schaefer and

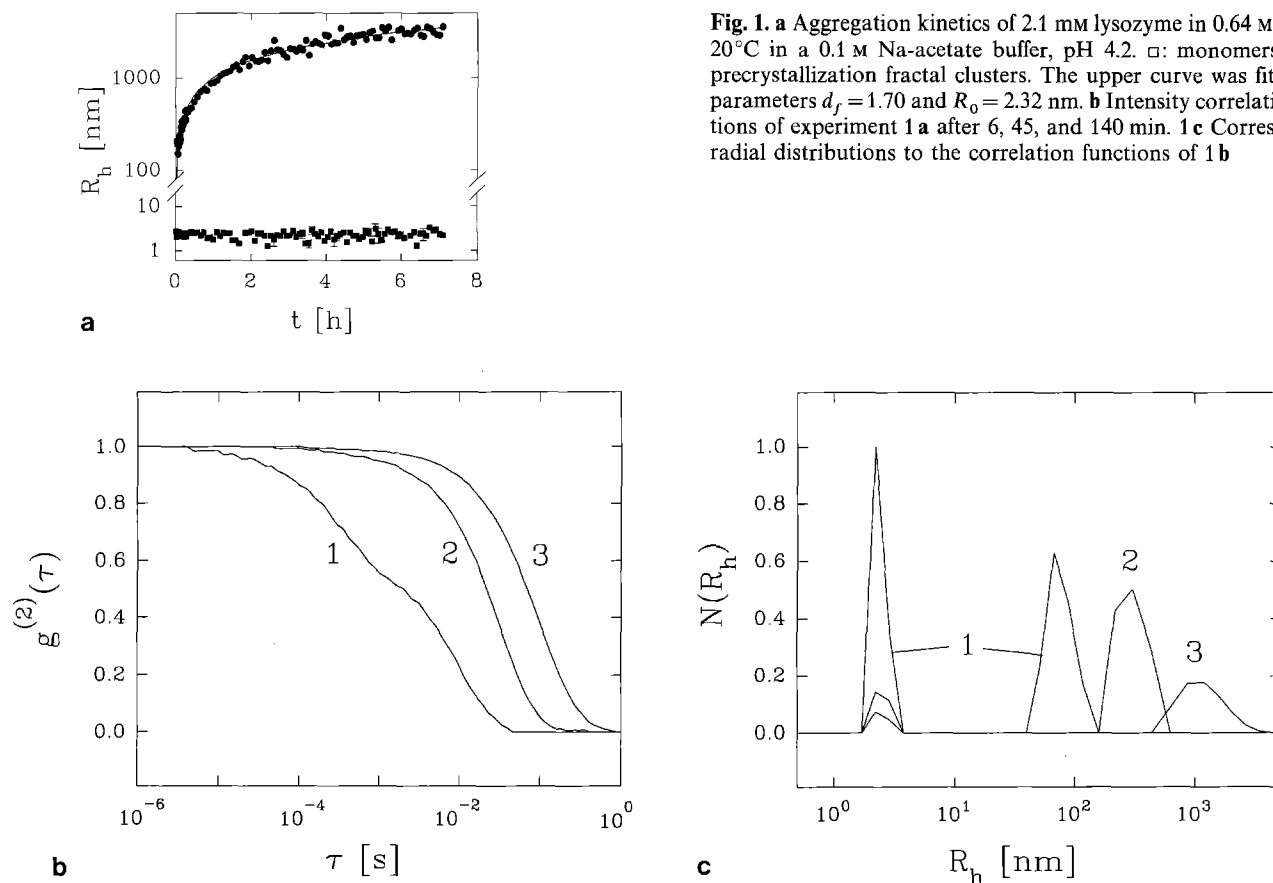


Fig. 1. a Aggregation kinetics of 2.1 mM lysozyme in 0.64 M NaCl at 20°C in a 0.1 M Na-acetate buffer, pH 4.2. □: monomers and ●: precrystallization fractal clusters. The upper curve was fitted with parameters $d_f = 1.70$ and $R_0 = 2.32$ nm. b Intensity correlation functions of experiment 1a after 6, 45, and 140 min. c Corresponding radial distributions to the correlation functions of 1b

Keefer 1987; Pusey and Rarity 1987)

$$\frac{M(t)}{M_0} = \left(\frac{R_g}{R_0} \right)^{d_f} \quad (14)$$

where M_0 and R_0 are the mass and the radius of the monomer, respectively, and R_g is the radius of gyration of the cluster. Lysozyme cluster having radii between 300–700 nm will be comprised of $7.8 \cdot 10^3$ – $3.6 \cdot 10^4$ monomers, assuming a fractal dimension of 1.8.

A 7 h duration kinetic experiment involving lysozyme in the presence of NaCl at 20°C is displayed in Fig. 1a. Radii and their standard deviations, obtained after analysis with CONTIN, are plotted in a logarithmic fashion against time. The first thirty spectra were sampled over 30 s whereas all others were over 5 min. The inverse Laplace transform resolves well both fractal clusters and monomers. The standard error associated with the cluster radii is small, less than 1.0%. The average monomer radius is 2.32 ± 0.34 nm, the fractal dimension of the clusters, calculated by a fit of (10) to the measured radii, is 1.70 ± 0.05 .

Selected correlation functions and the corresponding particle radius distribution are displayed in Figs. 1b, c. The correlation functions were collected 6, 45, and 140 min after initiation of the experiment. Whereas in the first function two decay times can be resolved, at later times the clusters dominate the spectra. Monomers can still be resolved in these cases, however the associated errors are larger.

Typical growth kinetics of lysozyme clusters with NaCl at 10°C and 50°C are shown in Fig. 2a. In either case, clusters are formed in the DLCA regime and exhibit fractal dimensions of 1.67 ± 0.17 and 1.60 ± 0.14 , respectively, obtained by non-linear fits according to (10). There is no significant dependence of the fractal dimension d_f on the temperature. The mean value obtained over the whole temperature range is $d_f = 1.69 \pm 0.23$ and agrees to within 7% with the universal value of 1.81 (Lin et al. 1989 a, b, 1990) for ideal colloidal gold aggregation in the DLCA regime. These departures should be treated with some caution since others (Olivier and Sørensen 1990; Asnaghi et al. 1992) have questioned the universal model of only two aggregation regimes and claim that a continuum of characteristic exponents could adequately describe fractal cluster formation.

Data collection when using $(\text{NH}_4)_2\text{SO}_4$ as a precipitating agent appears more difficult than with NaCl. In the beginning of each run several spectra had to be discarded owing to transients of large clusters through the scattering volume. These effects are in accord with an initial formation of large and rapid precipitating clusters. Later, the behavior changed to diffusion limited aggregation. The fractal dimensions determined after omitting the first ten to fifteen points from each curve are 1.79 ± 0.16 and 1.82 ± 0.10 , respectively. These values are in very good agreement with the value of 1.81 for DLCA aggregation.

The dependence of the overall scattered intensity upon the radius of the scatterers gives another way to obtain

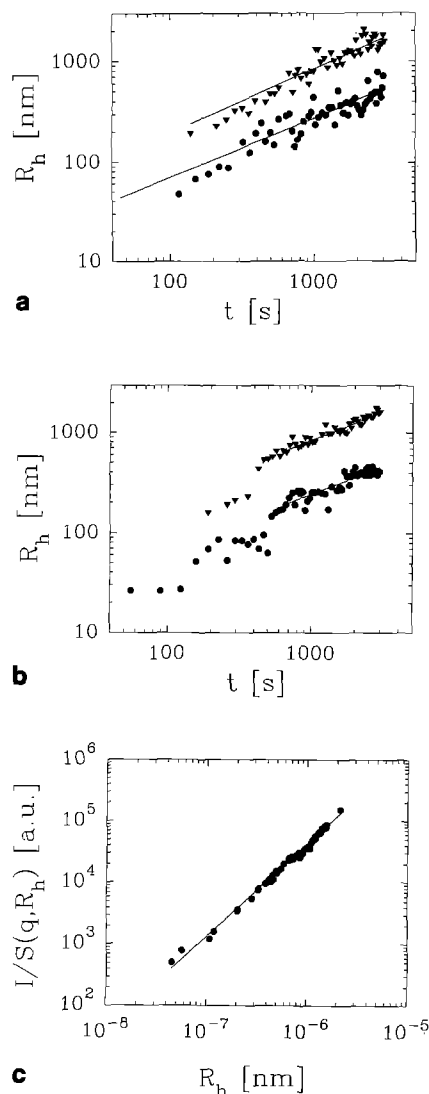


Fig. 2 a–c. Cluster aggregation kinetics of lysozyme in **a** NaCl and **b** in $(\text{NH}_4)_2\text{SO}_4$ at 10°C (●) and 50°C (▽), respectively. Fits to the DLCA regime calculated from Eq. (10) are shown. **c** Double logarithmic plot of scattered intensity divided by the static structure factor in arbitrary units as a function of the hydrodynamic radius. The solid line denotes the fitted slope with a fractal dimension of $d_f = 1.51 \pm 0.14$. Experimental conditions: 2.1 mM lysozyme with 0.64 M NaCl at 25°C

the fractal dimension of the scattering particles. The intensity is related to the hydrodynamic radius by a power law (Pusey and Rarity 1987)

$$I \propto R_h^{d_f} S(q, R_h), \quad (15)$$

furthermore the static structure factor $S(q, R_h)$ has to be taken into account, because of the size and the fractal nature of the clusters. In Fig. 2c a log-log plot of the scattered intensity divided by the static structure factor versus the hydrodynamic radius is shown, where the slope gives the fractal dimension. Aggregation of 2.1 mM lysozyme was initiated by 0.64 M NaCl at a temperature of 25°C. A linear regression analysis yields the fractal dimension as $d_f = 1.51 \pm 0.14$. This value is in between the error range of the value calculated from the aggrega-

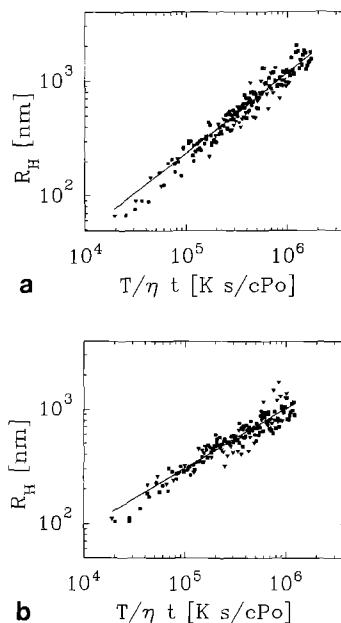


Fig. 3. a Scaled aggregation kinetics of 2.1 mM lysozyme with 0.64 M NaCl at 10°C (●), 30°C (▽), and 50°C (□). The curve shown in the figure is a fit to the data with a fractal dimension of $d_f = 1.62$. **b** Scaled aggregation kinetics of 2.1 mM lysozyme with 1.14 M $(\text{NH}_4)_2\text{SO}_4$ at temperatures of 20°C (●), 35°C (▽), and 50°C (□). The curve shown in the figure is a fit to the data with a fractal dimension of $d_f = 1.82$

tion kinetics, deviations may result from intensity which is scattered by the monomers.

Evaluation of experiments which were performed at different temperatures or with 1.14 M $(\text{NH}_4)_2\text{SO}_4$ as precipitating agent did not lead to diverging results.

3.2. Dynamic scaling of aggregation kinetics

A proof of the fractal nature of the aggregates is given in Figs. 3 a, b. When the elapsed times are normalized by T/η according to Eqs. (10) and (11) (Feder et al. 1984) all points should fall onto a universal master curve with a slope equal to the reciprocal of the characteristic fractal dimension.

Aggregation kinetics of 2.1 mM lysozyme with 0.64 M NaCl at temperature of 10°C, 30°C and 50°C are displayed in Fig. 3 a. Similarly, scaled aggregation kinetics of 2.1 mM lysozyme with 1.14 M $(\text{NH}_4)_2\text{SO}_4$ at temperatures of 20°C, 35°C and 50°C are displayed in Fig. 3 b. Intermediate temperatures exhibited comparable behavior for both precipitating agents, whereas it was not possible to scale the $(\text{NH}_4)_2\text{SO}_4$ data at temperatures below 15°C.

The universal scaling, despite small uncertainties due to minor concentration differences between the solutions studied indicates that an extension of the measured data in the intermediate and $qR \gg 1$ regimes is possible. It is successfully accomplished if the necessary precautions for the correct particle sizing are taken. Our results are at variance with the work of Feder et al. (1984) who determined a fractal dimension of 2.5 for immunoglobulin aggregation kinetics as a function of temperature and

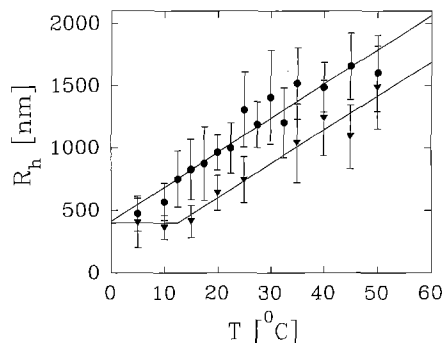


Fig. 4. Dependence of the quasi-stationary hydrodynamic radius of lysozyme fractal clusters on temperature in (●) 0.64 M NaCl and (▼) 1.14 M $(\text{NH}_4)_2\text{SO}_4$. The points indicate an average of three independent experiments

protein concentration in the $qR \ll 1$ regime. However, the lysozyme solution studied here is intrinsically more stable and better defined.

We conclude that the aggregation of lysozyme induced by NaCl follows DLCA, whereas $(\text{NH}_4)_2\text{SO}_4$ induced aggregation follows late cross-over 15°C behavior at comparable times. The aggregates formed in either case are perfect fractals a few minutes after initiating the reaction.

3.3. Temperature dependence of the cluster sizes

Averaged quasi-stationary radii as a function of temperature of three independent experiments are displayed in Fig. 4. Aggregation initiated by NaCl led to clusters with radii 480 ± 140 nm at 5°C and 1600 ± 307 nm at 50°C. The linear dependence of the cluster size on the temperature corroborates the view that growth of these clusters takes place in the DLCA regime. An increase of the thermal energy increases the rate of collision and growth of clusters is faster. The rate of cluster growth can be estimated as 28 nm/°C.

If lysozyme aggregation is initiated by addition of $(\text{NH}_4)_2\text{SO}_4$ the radii of the clusters do not exhibit a linear temperature dependence. Between 5 and 20°C radii fluctuate around 400 ± 30 nm. A transition is observed above 15°C and clusters grow to approximately 1500 ± 330 nm at 50°C. It seems that below room temperature the molecules cannot overcome the energy barrier. However, at higher temperatures, the barriers can be more easily overcome and the rate of collision increases. Above the transition temperature, the rate of cluster growth is comparable with that of the NaCl clusters, namely 27 nm/°C.

Lysozyme in the presence of $(\text{NH}_4)_2\text{SO}_4$ forms gels at initial temperatures higher than 20°C after two weeks. X-ray diffraction studies of the gels did not indicate the existence of microcrystalline structures. Gelation can be understood in terms of modification of the scaling exponents of the Smoluchowski collision kernel and concomitant changes of the particle size distribution (van Dongen and Ernst 1985 a, b; Ernst 1987). Despite its interesting properties, a systematic study of the gelling transition is out of the scope of the present work. However, these findings suggest that lysozyme can be directly involved in a wider spectrum of complex phenomena and provides

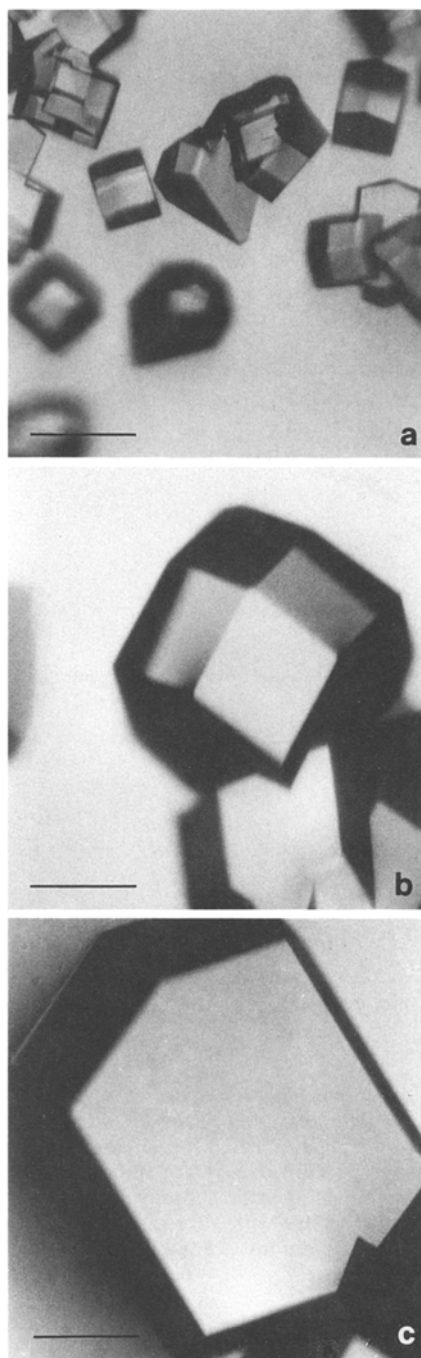


Fig. 5a–c. Lysozyme crystals grown from NaCl as a function of the starting aggregation temperature. Photographs are taken after 36 h under a magnification of 80 times. The temperature during the first 45 min of aggregation is **a** 5°C, and the crystal size 180 μm , **b** 25°C, crystal size 650 μm , and **c** 45°C, crystal size 820 μm . Bar size equals 250 μm

additional evidence for the fractal nature of the clusters involved in the crystallization process.

3.4. Correlations between cluster and crystal size

Since the only variable in the experiments described above is the temperature of the early aggregation stage

(during the first 50 min), it is worth examining in a qualitative way its effect on crystals grown within the next few days. In all experiments conducted in the presence of NaCl, a clear dependence of both crystal size and number, on starting temperature was observed.

Pictures of lysozyme crystals were taken through a light microscope 36 h after completion of the light scattering experiment. Experiments performed at a starting temperature of 5°C produced typical crystal sizes of about 180 µm, at 25°C of 650 µm, and at 45°C of 820 µm (Fig. 5a–c). The number of crystals present in the light scattering cells seems to follow a reciprocal temperature dependence and thus fewer crystals are detected at higher starting temperatures.

A dramatic increase in the crystal size was observed after incubating samples with a lower initial concentration, 1.45 mM, of lysozyme with 0.64 M NaCl and by applying a temperature gradient. Temperature was varied between 10–50–10°C with a rate of 0.5°C/min for the heating cycle and 0.25°C/min for the cooling cycle. Changes in temperature can be understood as changes of the solubility of the solution. It has been shown (Heinrichs et al. 1992) that exponential temperature gradients have marked effects on crystal growth. During one cooling and heating cycle growth was quenched and the cluster radii remained nearly constant to the end of the experiment. After completion of the experiments the samples were kept again at constant temperature. Crystals grew in less than 24 h and reached a maximum size of 2.2 mm within 72 h. The behavior can probably be explained by a ripening mechanism where the applied gradients seem to accelerate dissolution and growth rates. To our knowledge successful crystallization attempts of lysozyme at the high temperatures, as the ones employed in the present work, have not yet been reported by other groups.

These observations have a qualitative character but are reproducible. For a quantitative description, large populations of crystals have to be examined and distribution histograms of their dimensions and number have to be constructed during the growth process (Pusey and Naumann 1986; Zuck and Ward 1991) and further correlated with the early stage of the aggregation kinetics.

4. Conclusions

In the present work we have investigated the effect of starting temperature in the growth of protein crystallization aggregates. Advances dictated by contemporary colloid chemistry allow a realistic description of the PCS profiles in the intermediate scattering vector regime. The fractal exponents of clusters can be obtained with fair precision and their size can be deduced in a rapid fashion during the early stages of the aggregation reaction (i.e. within less than sixty min).

The temperature variation at the initial stage, whereas later solutions are allowed to relax, renature and restructure for several days at constant temperature, seems to be a very important factor. Dynamic scaling of the size of the clusters growing under optimal and suboptimal crystallization conditions is observed and either case can be

described by different collision processes that lead to either crystallization or gelation. At least for lysozyme, the probability that a global crystallization minimum is attained, is reinforced when aggregation takes place initially in the pure DLCA regime. In contrast, aggregation induced by addition of $(\text{NH}_4)_2\text{SO}_4$ takes place initially in the cross-over regime and leads to fractal clusters of smaller sizes at comparable times. The size of these clusters is independent of temperature up to 15°C, above this temperature clusters grow faster and gelation is completed within two weeks.

Precrystallization clusters are fractals characterized by fast DLCA aggregation, or late-cross-over behavior indicative of the onset of nucleation (Hoekstra et al. 1992), with a dimensionality close to 1.70. Since we have not observed growth of crystals, after extended periods of time, in the pure RLCA or early-cross-over regime we can identify those aggregates as precursors of a precipitation reaction. It is worthy noting that nearly all structures observed during the present study have been experimentally verified by small angle X-ray experiments in tetraethylorthosilicate (Schaefer and Keefer 1987). Therefore the identifications of pathways connecting the structure with the precursor growth process is not an intractable task.

A crucial question that is under investigations is whether and how these clusters are related to the nucleation process and further crystal growth. Nucleation kinetics of lysozyme have been observed for a limited number of cases only because it is very fast and cannot be captured by the PCS experiment. Therefore, a precise definition of critical radii as a function of solution supersaturation is very difficult under the conditions employed. Fractal cluster formation can be understood as a result of nuclei-nuclei collision whereas the exact border between nucleation and postnucleation events is not easy to define. We have good reasons to believe that fractal clusters are not random byproducts of unsuccessful nucleation but they serve for buffering concentration and charge, thus optimizing the degree of supersaturation of the solution.

One could imagine that the delayed cross-over behavior of $(\text{NH}_4)_2\text{SO}_4$ is associated with the formation of nuclei with smaller critical sizes than those formed by NaCl. Longer induction times may be very important for the success of a crystallization experiment. However, in both cases the fractal structures are involved in ordering processes such as gelation and crystal formation. The individual solvent mediated interaction pattern that lysozyme exhibits with each precipitating agent is responsible for the appearance of the two processes. The question of whether nuclei at the early states are compact or tenuous structures is also not easy to answer at this stage. Restructuring of tenuous structures could lead to compact ones with smaller sizes and higher fractal dimensions (Meakin 1988). Theoretical studies (Klein and Leyvraz 1986; Yang et al. 1990) have indicated nucleation models that may depart from the classical picture.

Acknowledgements. We thank the European Community, the Deutsche Forschungsgemeinschaft (Leibniz Award) and ESA/ESTEC for financial support. We also thank Dr. R. Gauglitz for making avail-

able his viscometry facilities and Mrs. C. Kisker for assistance with X-ray diffraction work.

References

- Asnaghi D, Carpineti M, Giglio M, Sozzi M (1992) Coagulation kinetics and aggregate morphology in the intermediate regimes between diffusion-limited and reaction-limited cluster aggregation. *Phys Rev A* 45 (2):1018–1023
- Ball RC, Weitz DA, Witten TA, Leyvraz F (1987) Universal kinetics of reaction-limited aggregation. *Phys Rev Lett* 3:274–277
- Boistelle R, Astier JP (1988) Crystallization mechanisms in solution. *J Cryst Growth* 90:14–30
- Chernov AA (1984) *Modern crystallography III*. Springer, New York
- Chu B (1991) *Dynamic light scattering*. Academic Press, New York
- Dongen PGJ van, Ernst MH (1985a) Cluster size distribution in irreversible aggregation at large times. *J Phys A: Math Gen* 18: 2779–2793
- Dongen PGJ van, Ernst MH (1985b) Dynamic scaling in the kinetics of clustering. *Phys Rev Lett* 13:1396–1398
- Ducruix AF, Ries-Kautt MM (1990) Solubility diagram analysis and the relative effectiveness of different ions on protein crystal growth. *Methods: A companion to methods in enzymology* 1:25–30
- Einstein A (1905) Über die von der molekularkinetischen Theorie der Wärme geforderte Bewegung von in ruhenden Flüssigkeiten suspendierten Teilchen. *Ann Phys* 17:549–560
- Einstein A (1906) Zur Theorie der Brownschen Bewegung. *Ann Phys* 19:371–381
- Ernst MH (1987) Kinetics of clustering. *Fractals in physics: Pietronero L, Tosatti E (eds)*. North Holland, Amsterdam, pp 289–302
- Feder J, Jøssang T, Rosenqvist E (1984) Scaling behaviour and cluster fractal dimension determined by light scattering from aggregating proteins. *Phys Rev Lett* 53:1403–1406
- Georgalis Y, Zouni A, Saenger W (1992) Dynamics of protein precrystallization cluster formation. *J Crystal Growth* 118:360–364
- Georgalis Y, Zouni A, Eberstein W, Saenger W (1993) Formation dynamics of protein precrystallization fractal clusters. *J Crystal Growth* 126:245–260
- Gilliland GL, Bickham DM (1990) The biological macromolecules crystallization database. *Methods: A Companion to Methods in Enzymology* 1: 6–11
- Heinrichs W, Heinrichs M, Schönert H-J (1992) Growth of protein single crystals in a periodically changed solubility gradient. *J Crystal Growth* 122:186–193
- Hoekstra LL, Vreeker R, Agterof WGM (1992) Aggregation of colloidal Nickel hydroxycarbonate studied by light scattering. *J Colloid Interface Sci* 151(1):17–25
- Klein W, Leyvraz F (1986) Crystalline nucleation in deeply quenched liquids. *Phys Rev Lett* 57(22):2845–2848
- Klein R, Weitz DA, Lin MY, Lindsay HM, Ball RC, Meakin P (1990) Theory of scattering from colloidal aggregates. *Progr Colloid Polymer Sci* 81:161–168
- Kolb M (1991) Aggregation phenomena. In: Gans W, Blemen A, Aman A (eds). *Large-scale molecular systems*, NATO ASI Series B: Physics, Vol 258. Plenum Press, New York, pp 231–251
- Lin MY, Lindsay HM, Weitz DA, Ball RC, Klein R, Meakin P (1989a) Universality of fractal aggregates as probed by light scattering. *Proc R Soc London A* 423:71–87
- Lin MY, Lindsay HM, Weitz DA, Ball RC, Klein R, Meakin P (1989b) Universality in colloidal aggregation. *Nature* 339:360–362
- Lin MY, Klein R, Lindsay HM, Weitz DA, Ball RC, Meakin P (1990a) The structure of fractal colloidal aggregates of finite extent. *J Colloid Interface Sci* 137:263–280
- Lin MY, Lindsay HM, Weitz DA, Ball RC, Klein R, Meakin P (1990b) Universal diffusion-limited colloid aggregation. *J Phys: Condens Matter* 2:3093–3113
- Lindsay HM, Klein R, Weitz DA, Lin MY, Meakin P (1988) Effect of rotational diffusion on quasielastic light scattering from fractal colloid aggregates. *Phys Rev A* 38:2614–2626
- Lindsay HM, Klein R, Weitz DA, Lin MY, Meakin P (1989) Structure and anisotropy of colloid aggregates. *Phys Rev A* 39:3112–3119
- Martin JE, Ackerson BJ (1985) Static and dynamic structure from fractals. *Phys Rev A* 31:1180–1182
- Martin JE, Leyvraz F (1986) Quasielastic-scattering linewidth and relaxation times for surface and mass fractals. *Phys Rev A* 34: 2346–2349
- Meakin P (1988) Fractal aggregates and their fractal measures. *Phase transitions and critical phenomena* 12. Domb C, Lebowitz JL (eds). Academic Press, New York, pp 351–489
- Olivier BJ, Sørensen CM (1990) Variable aggregation rates in colloidal gold; Kernel homogeneity dependence on aggregant concentration. *Phys Rev A* 41(4):2093–2100
- Provencher SW (1982a) A constrained regularization method for inverting data represented by linear algebraic or integral equations. *Comput Phys Commun* 27:213–228
- Provencher SW (1982b) CONTIN: A general purpose constrained regularization program for inverting noisy linear algebraic and integral equations. *Comput Phys Commun* 27:229–242
- Pusey M, Naumann R (1986) Growth kinetics of tetragonal lysozyme crystals. *J Cryst Growth* 76:593–599
- Pusey PN, Rarity JG (1987) *Mol Phys* 62:411–418
- Rarity JG, Seabrook RN, Carr RJG (1989) Light-scattering studies of aggregation. *Proc R Soc Lond A* 423:89–102
- Ries-Kautt MM, Ducruix AF (1989) Relative effectiveness of various ions on the solubility and crystal growth of lysozyme. *J Biol Chem* 263:745–748
- Rosenberger F (1986) Inorganic and protein crystal growth – similarities and differences. *J Cryst Growth* 76:618–636
- Schaefer DW, Keefer KD (1987) Structure of random silicates. *Fractals in physics: Pietronero L, Tosatti E (eds)*. North Holland, Amsterdam, pp 39–53
- Schätzel K (1993) Photon correlation spectroscopy, the method and some applications. Brown W (ed). Oxford University Press, Oxford
- Schulz-Dubois EO (ed) (1983) *Photon correlation techniques in fluid mechanics*. Springer, New York
- Siegert AJF (1943) MIT Lap Rep No 465–470
- Schmitz KS (1990) *An introduction to dynamic light scattering by macromolecules*. Academic Press, New York
- Smoluchowski M von (1916) Drei Vorträge über Diffusion, Brownsche Molekularbewegung und Koagulation von Kolloidteilchen. *Physik Z* 17:557–599
- Smoluchowski M von (1917) Versuch einer mathematischen Theorie der Koagulationskinetik kolloidaler Lösungen. *Z Physik Chem* 2:129–168
- Verwey EJW, Overbeek JTG (1948) *Theory of the stability of lyophobic colloids*. Elsevier, Amsterdam
- Vicsek T (1989) *Fractal growth phenomena*. World Scientific, Singapore
- Weitz DA, Lin MY (1986) Dynamic scaling of cluster mass distribution in kinetic colloid aggregation. *Phys Rev Lett* 16:2037–2040
- Weitz DA, Huang JS, Lin MY, Sung J (1984) Dynamics of diffusion-limited kinetic aggregation. *Phys Rev Lett* 17:1657–1660
- Yang J, Gould H, Mountain RD (1990) Molecular dynamics investigation of deeply quenched liquids. *J Chem Phys* 93(1):711–723
- Zuck WM, Ward KB (1991) Methods of analysis of protein crystal images. *J Cryst Growth* 110:148–155